

PROGRESSIVE COLLAPSE ANALYSIS OF 2-D RC FRAMES USING AEM

Osama El-Mahdy¹, El-Sayed El-Kasaby², Hala Abusafa², Amr El-Gama²

1. *Department of Civil Engineering, Faculty of Engineering at Shoubra, Benha University, Shoubra, Cairo, Egypt*
2. *Department of Civil Engineering, Benha Faculty of Engineering, Benha University, Benha, Egypt, amr.ali@bhit.bu.edu.eg, engamrramadan@yahoo.com*

ABSTRACT

Numerical simulation of a progressive collapse of structures using computer has a very actual apprehension for structural engineers due to their interest in structures veracity estimation. This simulation helps engineers to develop methods for increasing or decreasing the progressive failure. Finite Element Method (FEM) is the most computer simulation analysis currently used to perform a structural vulnerability assessment. Unfortunately, FEM is not able to automatically analyze a structure after element separation and collision which has a great effect on a structure's performance during collapse. For instances, a bombing load can cause damage to a main supporting column in a structure, which will cause debris flying at a very high velocity from the damaged column. This debris can cause another local failure in another column upon impact and lead to the progressive collapse of the whole structure. A new simulation technique, which was developed in 1995 as part of Tagel-Din's doctoral research, called Applied Element Method (AEM) can simulate the structure's behaviour from zero loading until collapse, through the elastic phase, opening and propagation of cracks, yielding of reinforcement bars and separation and collision of elements. This method is used in Extreme Loading for Structures software (ELS) by Applied Science International (ASI). In the current paper, a brief description of the AEM is given. Also, numerical modelling based on two experimental studies available in the literature conducted by Ahmadi et al. [1] and Yi et al. [2] are generated using ELS. These models are used to confirm the capability of AEM in simulation the progressive collapse behaviour of structures. Also, the models are utilized to examine and measure the structural resisting mechanisms of reinforced concrete structures against progressive collapse. The obtained numerical results indicated that, ELS can accurately model all structural behaviour stages up to collapse. A better agreement between the experimental and numerical results is observed. Moreover, the results obtained with ELS indicated an enhanced agreement with other software packages such as; OpenSees, Ansys, Abacus, and MSC Marc.

KEYWORDS

Progressive collapse, Reinforced concrete frames, Applied element method, Extreme loading for structures, Displacement control

1. INTRODUCTION

The prevention of progressive collapse lies primarily in the appropriate and effective analysis of the structures having high potential to progressivity. To minimize the progressive collapse risks, the structural system of the building should be able to bear the removal of one or more structural elements and redistribute their loads on the neighbouring elements, so that disproportionate collapse would not take place.

Many definitions for progressive collapse phenomenon are given in buildings codes and standards such as ASCE 7-05 [3] and GSA [4]. Other definitions can be found in the related literature such as Nair [5] and Ellingwood & Dusenberry [6].

Progressive collapse of a building could be caused by man-made accidental extreme loadings such as car accident, explosion of gas or steam services system, or an aircraft crash. The failure of the structural member can be also due to intentional loading that aims the structure failure like using a bomb in a criminal or structure demolition. Another cause for the structural component loss is natural hazards like hurricanes, tornados, floods, fires, or earthquakes. Mistakes in design and construction or overload due to change of use or structural modifications can also lead to structurally significant abnormal loadings.

Because of such collapses, many international structural codes and standards started to consider the progressive collapse resistance that help owners, developers, and engineers in designing building facilities for withstanding progressive collapse effect. These codes and standards differ in dealing with the progressive collapse in different ways such as the definition of progressive collapse, the used load combination, consideration of lateral load, approaches for progressive collapse threshold, and acceptance criteria. Among the codes that discussed the issue of progressive collapse are the Interagency Security Design Committee (ISC) [7], the British standards (BS 5950-1) [8], the General Services Administration (GSA) published in 2003 [4], and the Unified Facilities Criteria (UFC) by Department of Defense, USA published in 2005 and 2009 [9]. However, regardless of the level of protection of the building, progressive collapse prevention should be achieved to allow for timely evacuation of the tenant to save lives.

Design codes use direct and indirect design methods for protection against progressive collapse. The indirect design method prevents progressive collapse by providing a minimum level of strength, continuity and ductility of the structure. The direct design method explicitly considers resistance to progressive collapse during the design process. ASCE7-05 [3] has proposed specific local resistance (SLR) and alternative load path (ALP) methods for direct designs. SLR requires that the building, or parts of the building, provide sufficient strength to resist load. In this method, the strength and ductility of critical elements can be determined during the design process. On the other hand, ALP allows local failure of structural members; however, it prevents extensive structural failure by providing an alternative load path. When a structural member fails, the energy stored in the damaged structural members is released and causes additional loading on the other structural members, which changes the load transmission paths. If the adjacent structural member has enough capacity and ductility to bear the additional load, the structural system forms an ALP to transfer the load. This method analyses the building under the effect of one or more structural elements removal. The major advantage of this method is that it is independent of the cause of failure and analysis can be applied to any threat for collapse of an element. In conventional methods of design, only the flexural mechanism is considered as an ALP, and compression arch action (CAA) and catenary action (CA) are beyond the scope of the design codes. CAA is a mechanism of resistance to vertical loads through the development of axial compressive force in beams. Development of this axial force requires the restriction of longitudinal deflection of beams by other members of the frame. CA is resistant to vertical loads through the development of tensile force in the horizontal members. Development of tensile force in beams requires a large deformation in the beam and the ability to create longitudinal restriction to balance this force.

Computer simulation is an important tool in determining the performance of structures in extreme loading conditions. The numerical methods used in structural analysis can be classified into two categories. In the first category, the model is based on continuum material equations. On the other hand, the second category can be defined using discrete element techniques, such as the extended distinct element method (EDEM). The finite element method (FEM) is the most common example for the first category, with the division of the domain into finite elements with the respective material properties. The FEM yields good results for structural analysis before collapse, even if one considers non-linear materials and geometry. However, if the structure's behaviour advances to a discrete state, because of crack opening and propagation, the FEM loses its efficiency. Discrete element techniques which allow the mechanical interaction between elements and can simulate the cracking process more easily when compared to FEM, depending on the size, shape and arrangement of the elements. Despite its advantages, in small displacement analysis, the EDEM is less accurate than the FEM and the analysis time is quite large for a reasonable number of elements that simulate real problems.

To overcome the EDEM's drawbacks, Tagel-Din and Meguro developed the Applied Element Method (AEM) which is adopting the discrete cracking approach. The major advantage of the AEM is its capacity to simulate different collapse modes of structures and the structure's behaviour from zero loading until collapse, including the elastic phase, opening and propagation of cracks, yielding of reinforcement bars and separation and collision of elements. However, the computation time required to simulate large structures' behaviour from zero loading until collapse might become very large due to the necessity of small time increments, to ensure numerical stability (Meguro and Tagel-Din [10-12] and Tagel-Din and Meguro [13-15]).

In this regard, one of the main advantages of the applied element technique is its capability of modelling, with high accuracy, both continuum and discrete phases of structural response. Figure 1 compares the performance of this method with respect to finite element techniques in terms of accuracy in a wide range of modelling capabilities.



Fig. 1 - Analysis domain of AEM (ASI [16])

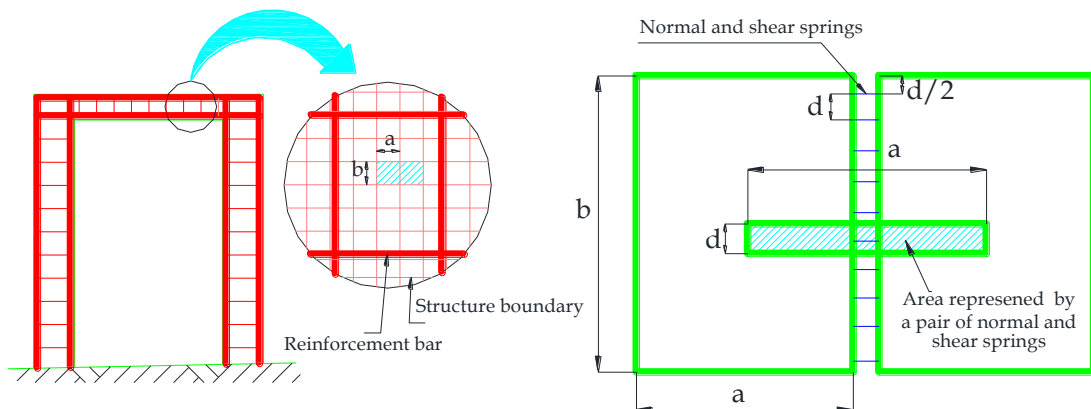
2. OBJECTIVE

The objective of this paper is to verify the capability of AEM in simulating the progressive collapse of two-dimensional reinforced concrete frames. Two experimental studies conducted by Ahmadi et al. [1] and Yi et al. [2] are modelled using the Extreme Loading for Structures (ELS) software. The obtained results are compared with those measured in the experimental works and predicated using other software package such as OpenSees, Ansys, Abacus and MSC Marc. Furthermore, the presented analytical model will lead to investigate and quantify the structural resisting mechanisms of reinforced concrete structures against progressive collapse.

3. BRIEF DESCRIPTION OF THE APPLIED ELEMENT METHOD (AEM)

The Applied Element Method (AEM) has been developed by Tagel-Din and Meguro [13] to create a link between the advantages of finite element method for continuum mechanics and discrete element method for discrete mechanics. Since then, the method was applied and verified for; elastic analysis, reinforced concrete structures subjected to cyclic loads and buckling and post-buckling behaviour (Meguro and Tagel-Din, [10-12]). Also, AEM was applied for crack initiation and propagation, estimation of failure loads of reinforced concrete structures, non-linear dynamic analysis of structures subjected to collisions and severe earthquakes (Tagel-Din and Meguro [13, 29 & 50]), fault-rupture propagation (Ramancharle et al. [17]), non-linear behaviour of brick structures (Mayorca and Meguro [18]) and blast analysis (Asprone et al. [19] and Coffield & Adeli [20]).

In the AEM, the structure is discretized into series of virtually relatively small rigid elements, with special shape and determined dimensions connected together along their faces through a set of three non-linear contact springs (one normal spring and two shear springs), which represent the continuity between elements and reflect the properties of the material characteristics used (concrete and reinforcement bars), and that is differ from the connectivity in FEM where the elements are connected by nodes, as shown in Figure 2. The springs located at contact points represent stresses, strains and deformations of a certain portion.



(a) Element generation for AEM (b) Spring distribution and area of influence of each pair of springs

Fig. 2 - Modelling in AEM (Meguro and Tagel-Din [10])

Each single element has six degrees of freedom; three for translations and three for rotations. Relative translational or rotational displacements between two neighbouring elements cause stresses in the springs located at their common face as shown in Figure 3.

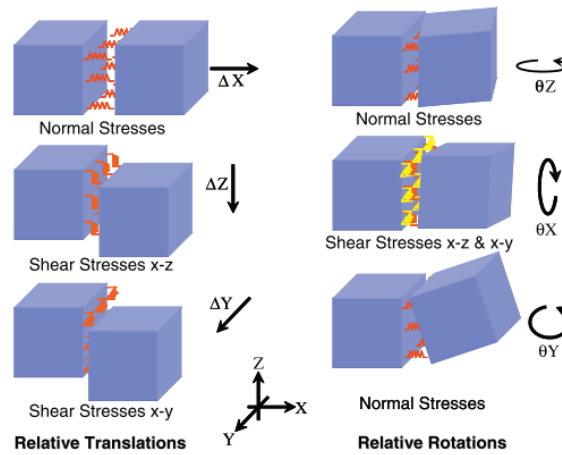


Fig. 3 - Stresses in springs due to elements' relative displacements (Applied Science International [21])

The AEM is a stiffness-based method, in which the stiffness of each pair of normal and shear springs connecting the element centerlines of an area ($d \times t$) with the length of “ a ” is calculated using Equations 1 and 2 (Meguro and Tagel-Din [10])

$$K_n = \left(\frac{E \times d \times t}{a} \right) \tag{1}$$

$$K_s = \left(\frac{G \times d \times t}{a} \right) \tag{2}$$

where, K_n is the stiffness of normal spring; K_s is the stiffness of the shear spring; d is the distance between the springs; t is the element thickness; a is the length of the representative area; and E & G are the Young's modulus and the shear modulus of the material, respectively.

Additionally, one must consider the element rotation, which is resisted by shear and normal springs. It is possible to calculate the theoretical rotational stiffness K_r from normal springs as follows:

$$K_r = \int_{-b/2}^{b/2} \frac{Et}{b} Z^2 = \frac{Etb^2}{12} \tag{3}$$

where, b the element's height and Z the spring's distance to the element centroid as represented in Figure 4. Therefore, it is possible to obtain the element's rotational stiffness as the sum of each spring's rotational stiffness, which leads to (Meguro and Tagel-Din [10]):

$$K_r = \frac{Etb^2}{4n^3} \sum_{i=1}^n \left(i - \frac{1}{2} \right)^2 \tag{4}$$

where $2n$ is the number of springs and i the spring number.

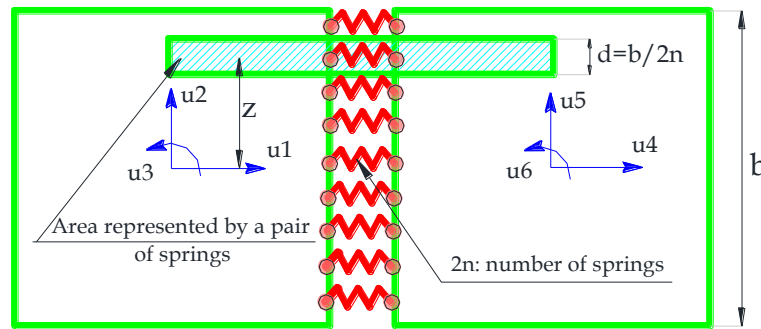


Fig. 4 - Normal springs for rotational stiffness (Meguro and Tagel-Din [10])

In the reinforced concrete model, two types of springs are used namely; matrix springs for concrete, and reinforcement springs for steel bars, as shown in Figure 5. Reinforcement springs can be set at the exact location of the steel bars so that all reinforcement details and amounts can be easily considered. In the case of the reinforcement spring, the representative area ($d \times t$) is replaced by the reinforcement bar area.

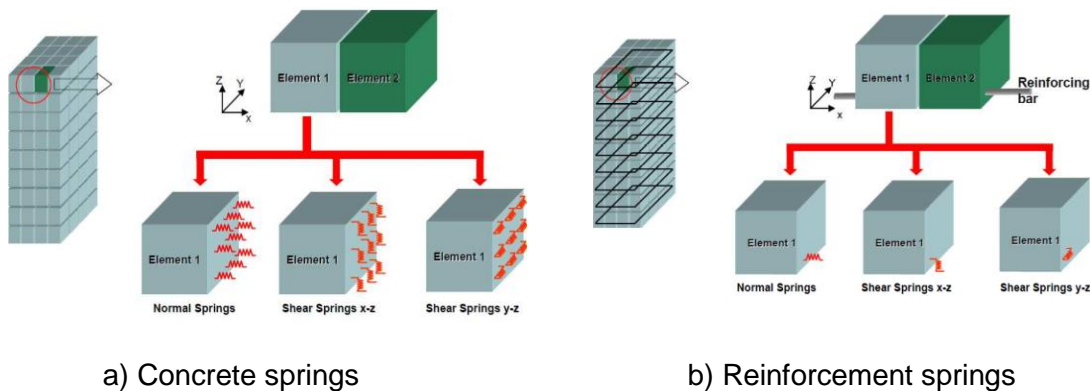


Fig. 5 - Concrete and reinforcement springs (Applied Science International [21])

In reinforced concrete structure, the matrix springs are cut or removed when the average tensile strain between two adjacent faces reaches the value of the separation strain, specified in the material properties of the model, and the element behaves as separate bodies for the rest of the analysis. Similarly, the reinforcement springs are cut off if the normal stress is equal or greater than the ultimate stress specified for this material or when the concrete spring cut even if the reinforcement springs have compression forces.

Although the reinforcement spring and the neighbouring concrete spring have the same strain, relative displacements can occur between reinforcement bars and the surrounding concrete, due to the assumption that the failure of concrete springs occurs prior to the failure of reinforcement springs (Applied Science International [21]).

In two-dimensional model, each element has three degrees of freedom and the size of the element stiffness matrix is (6 x 6). The element stiffness matrix is determined based on the relative coordinates between the location of the contact points and the element centerline and on the spring stiffness, as shown in Figure 6. On the other hand, in three-dimensional model, every element has six degrees of freedom. Therefore, a (12x12) stiffness matrix is generated (Meguro and Tagel-Din [11]). The element stiffness matrix depends on the spring material and status, for example, it considers whether the spring is for steel or concrete. In case of concrete, it considers

whether the spring is already cracked or reached compressive failure criteria. In case of steel, it also follows the constitutive stress-strain relations. These elements matrices are assembled at the structural master stiffness matrix.

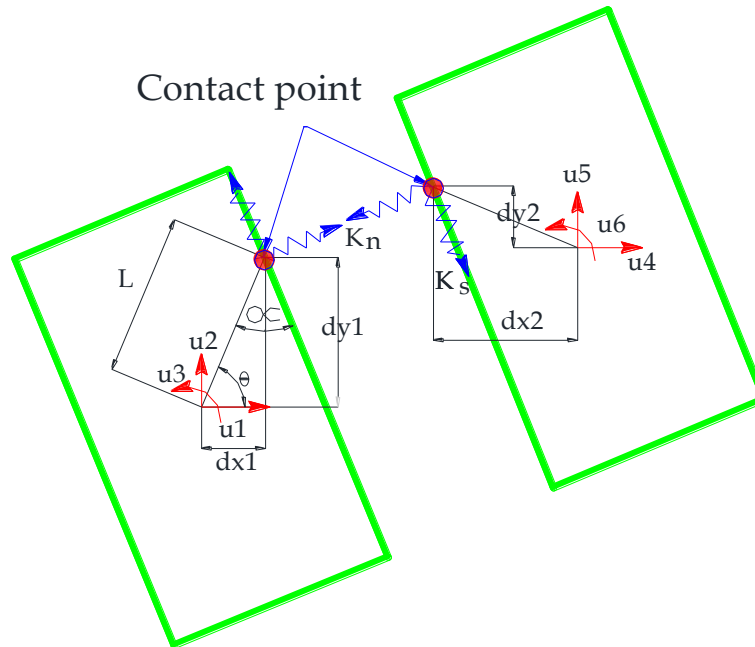


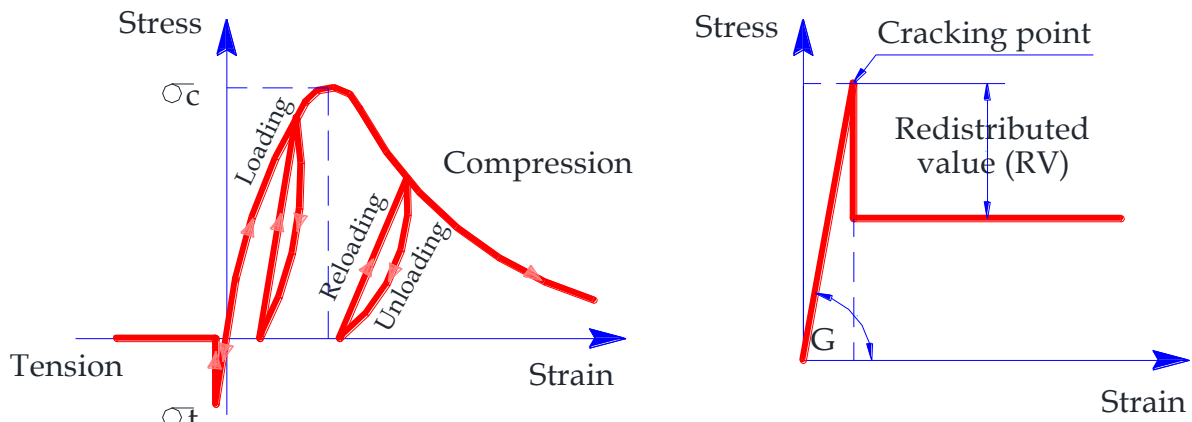
Fig. 6 - Element shape, contact point and DOF (Meguro and Tagel-Din [11])

In the AEM, fully non-linear path-dependent constitutive models are adopted for concrete and reinforcement bars as shown in Figure 7. The Maekawa compression model, an elasto-plastic and fracture model, is utilized for concrete in compression (Okamura and Maekawa [22]). While for concrete in tension, a linear stress-strain relationship is used until reaching the cracking point, then the stresses drop to zero. The residual stresses are then redistributed in the next loading step by applying the redistributed force values in the reverse direction. Also, the relationship between the shear stress and shear strain is assumed to be linear until the cracking of the concrete and the level of drop of shear stresses depends on the aggregate interlock and friction at the crack surface.

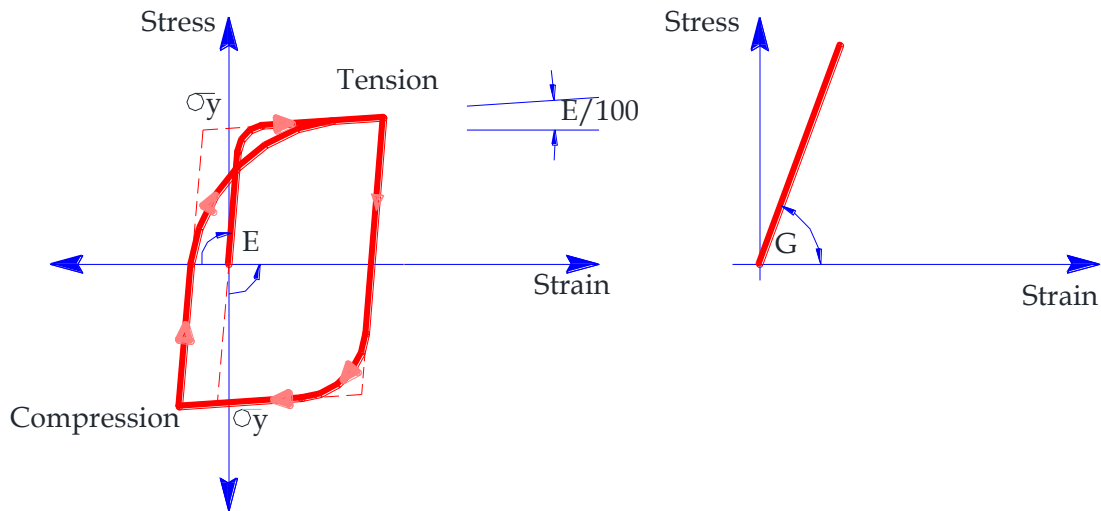
The transverse reinforcement confines the concrete and increases compressive strength. To consider the biaxial confinement effects in compression zones, Kupfer biaxial failure function is adopted. A modified compressive strength, f_{ceq} , is calculated as a function of the principal stress components (σ_1 and σ_2) and the compression stress f_c as follows (Kupfer et al. [23]):

$$f_{ceq} = \frac{1 + 3.65(\sigma_1/\sigma_2)}{[1 + \sigma_1/\sigma_2]^2} f_c \quad (5)$$

This indicates that the compressive resistance associated with each spring is variable and depends mainly on the stress situation at the spring location.



(a) Tension, compression and shear models for concrete [22]



(b) Reinforcement under axial and shear stresses [24]

Fig. 7 - Constitutive models for concrete and steel

For reinforcement bars, the model presented by Ristic et al. [24] is adopted. The stiffness of the steel spring after yielding is set to 1% of the initial spring stiffness. The tangent stiffness of reinforcement is calculated based on the strain from the reinforcement spring, loading status (either loading or unloading) and the previous history of steel spring which controls the Bauschinger's effect. The main advantage of this model is that it can consider easily the effects of partial unloading and Bauschinger's effect without any additional complications to the analysis. It should be emphasized that, some other failure phenomena like buckling of reinforcement and spalling of concrete cover, are not considered in the analysis yet.

To account for large displacements, the following modification to Equation 6 is introduced (Meguro and Tagel-Din [12]):

$$K\Delta u = \Delta f + R_M + R_G \tag{6}$$

where K is the non-linear stiffness matrix, Δu the incremental displacement vector, Δf the incremental load vector, R_G is the residual load vector due to geometric changes in structure during loading and R_M is the residual load vector due to cracking or incompatibility between spring stress and the corresponding strain.

The equilibrium equations represent a linear system of equations for each step. The solution of the equilibrium equations is commonly solved using Cholesky upper-lower decomposition. Separated elements may collide with other elements. In that case, new springs are generated at the contact points of the collided elements.

Modelling a progressive collapse mechanism should begin with the whole of structure elements then, specify the structural elements that will be instantaneously removed. However, most programs are incapable of analysing the change in their geometry and stiffness matrices. A more advanced software package was developed using the theory of AEM. This software is called Extreme Loading for Structures (ELS), and will be used in this paper.

4. VALIDATION OF AEM USING ELS SOFTWARE

Literature has shown that AEM gives good estimations for large displacements of structures undergoing collapse (Galal and El-Sawy [25], Meguro and Tagel-Din [10 & 11], Sasani [26], Wibowo et al. [27], Tagel-Din and Rahman [28], Tagel-Din and Meguro [15 & 29], Salem [30], Tagel-Din [31], Meguro and Tagel-Din [32], Park et al. [33], Helmy et al. [34 - 36], Salem and Helmy [37], Salem et al. [38 & 39], Lupoae and Bucur [40], Lupoae et al. [41] and El-Mahdy et al. [42]).

Experimental tests conducted by Ahmadi et al. [1] and Yi et al. [2] are modelled using ELS (v. 2.3) software to validate the AEM. However, sensitivity analysis for mesh, springs, loading steps, and calibration of the constitutive models should be done firstly.

4.1 Sensitivity analysis

A mesh sensitivity analysis is performed for the experimental works to study the effect of element size and the number of connecting springs between elements. The experiments are analysed using three increasingly smaller-sized elements (approximately cubic shapes with edges of 100, 50 and 25 mm). Additionally, for each different element size, two models are considered, using 5 and 10 connecting springs for each pair of adjacent element faces. The convergence is considered achieved when the changes in the load-displacement result from one analysis to the next are too small to be visually noticeable. As shown in Figures 8 and 9, the estimation for load-displacement is achieved for a mesh of edge of 50 mm and 5 connecting springs between element faces and therefore, this combination is considered an appropriate mesh and used for the tests reported in this paper. A similar analysis is performed to calibrate the loading increment on model. Load-displacement curves are obtained using 0.10, 0.50, 1.00, 1.50, 2.00 mm loading steps and no noticeable differences were obtained between the resulting capacity curves. So, for all experiments, a step of 1.00 mm is used.

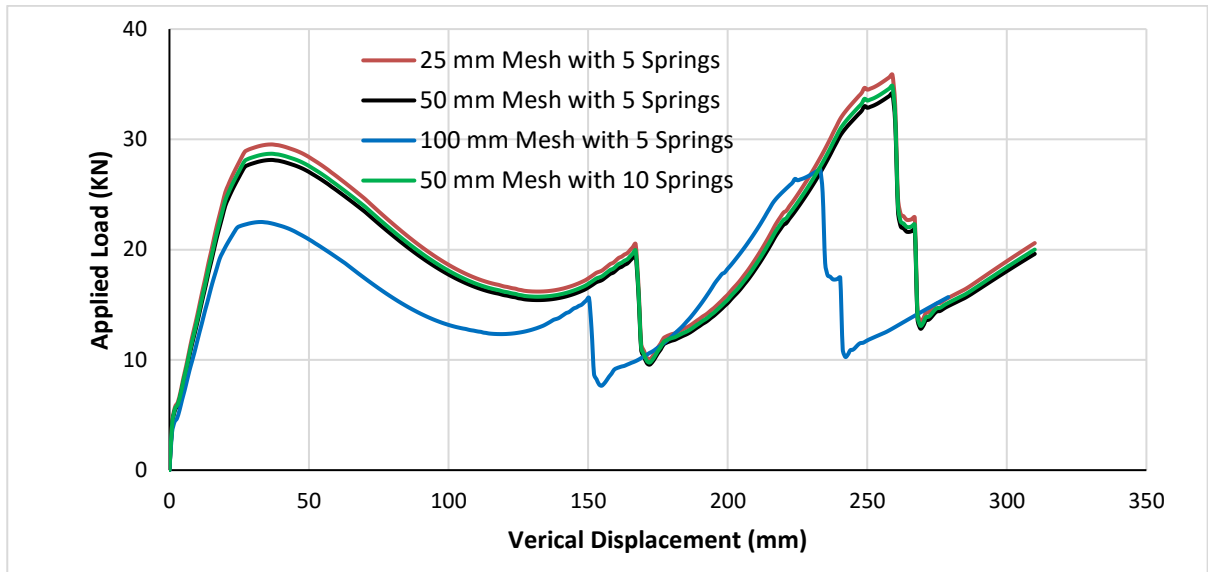


Fig. 8 - Effect of element size and the number of connecting springs between elements for Experimental work by Ahmadi et al. [1]

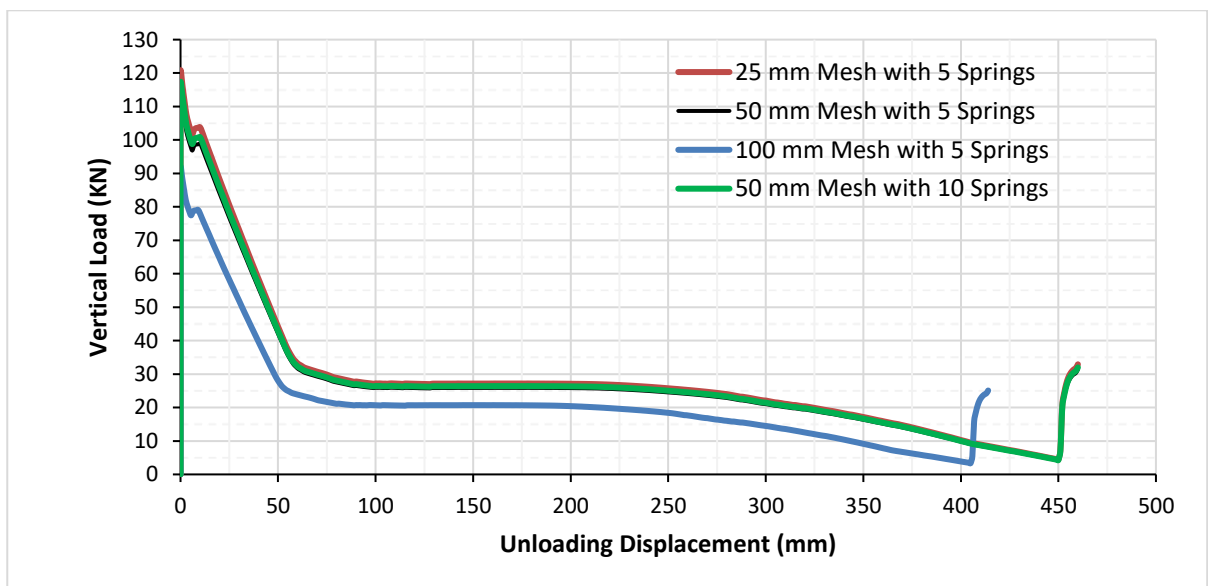


Fig. 9 Effect of element size and the number of connecting springs between elements for Experimental work by Yi et al. [2]

4.2 Calibration of the constitutive models

4.2.1 Steel

Due to lack of information for steel stress-strain curves in the experiments, the material characterization under tensile tests were simulated numerically and used to calibrate the parameters defining the Ristic constitutive model of steel (Ristic et al. [24]). The mechanical properties presented in each experimental were used, considering Young's modulus and shear modulus presented in each experimental and a post yield stiffness factor of 0.01.

4.2.2 Concrete

The characteristic compressive strength (f_{ck}), the modulus of elasticity (E_c) and the tensile strength of the concrete (f_{ct}) were calculated from its compressive strength according to Equations. 7 to 9 (FIP Model Code [43]). The concrete shear modulus is taken as $E/2(1+\nu)$ and a Poisson ratio (ν) of 0.2 is considered.

$$f_{ck} = f_c - 8 \text{ (MPa)} \quad (7)$$

$$E_c = 21.5 \left(\frac{f_c}{10} \right)^{1/3} \text{ (GPa)} \quad (8)$$

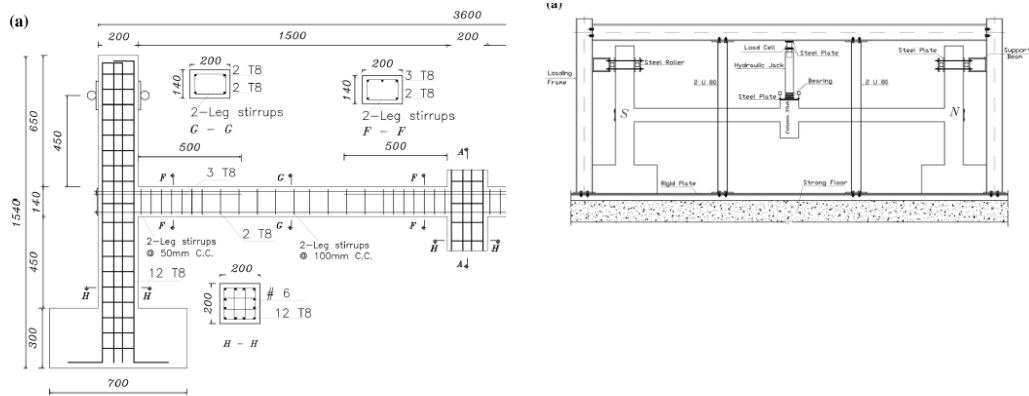
$$f_{ct} = 0.3(f_{ck})^{2/3} \text{ (MPa)} \quad (9)$$

Another important parameter characterizing the material constitutive models in ELS is the separation strain. This parameter defines the strain value in the springs located between two neighbouring elements at which the elements are considered to be physically separated. According to the ELS Modelling Manual (ASI [21]), for reinforced concrete elements, the separation strain should be higher than the ultimate tensile strain of the reinforcement bar.

4.3 Experimental work by Ahmadi et al. [1]

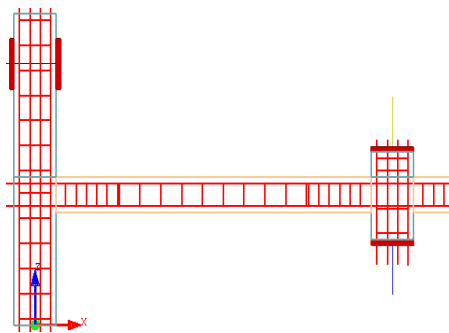
4.3.1 Experiment description

Ahmadi et al. [1], performed an experimental and numerical evaluation using the OpenSees open-source platform as part of a research program to examine progressive collapse of structures under column removal scenario at Iran University of Science and Technology (IUST). The aim of this work was to investigate the alternative load paths and resistance mechanisms in scaled sub-assembly and to compare the differences between the results of full-scale and scaled specimens. The full-scale assembly was selected from a 10-story office building which was designed based on an intermediate moment frame (IMF) system. The building was analysed based on the dead, live, and earthquake loads defined in ASCE7-05 [3] and designed based on ACI 318R-02 [44]. The specimen included two single-bay beams, one middle joint (a middle column stub), and two end columns with foundations to behave as two-dimensional specimen. The specimen was fastened to a displacement control point loaded (a monotonic vertical load) above the middle column stub to simulate the progressive collapse of the frame. The test continued until complete failure of the specimen. During testing, alternative load paths, mechanism of formation and development of cracks, corresponding displacements and strains at predefined points and sections were measured and the formation of resistance mechanisms and failure modes were recorded. The dimensions, reinforcement details of the specimen components, and test setup are shown in Figure 10. Furthermore, measured material properties are given in Tables (1 and 2). The researchers found that, load-displacement curve, mechanism of formation and development of cracks and failure mode of the scaled specimen had good agreement with the full-scale assembly. Also, they found that macro-model can provide a good estimation of collapse behaviour of RC sub assembly under the middle column removal scenario.

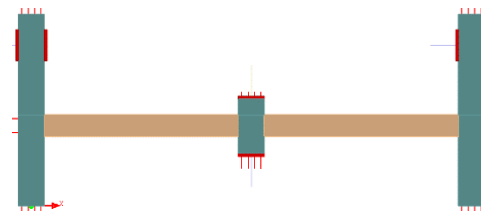


(a) Dimensions and reinforcement for the specimen (half part only) [1]

(b) Test setup [1]



(c) Modelling in ELS (half part only)



(d) Modelling in ELS

Fig. 10 - Specimen details and numerical modeling

Tab.1 - Concrete material properties (Ahmadi et al. [1])

Property	Young's Modulus (MPa)	Shear Modulus (MPa)	Tensile Stress (MPa)	Average Compressive stress (MPa)	Specific Weight (Kg/m ³)	Ultimate Strain
Concrete	2.610E4	1.0210E4	1.5	26	2500	0.20

Tab. 2 - Reinforcement material properties (Ahmadi et al. [1])

Property	Young's Modulus (MPa)	Shear Modulus (MPa)	Tensile and Compressive Yield Stress (MPa)	Ultimate Stress (MPa)	Specific Weight (Kg/m ³)	Ultimate Strain
T8	2.010E5	8.010E4	530	650	7840	0.16

4.3.2 Modelling and simulating

In the present paper, the tested specimen is modelled using ELS. Meshing division and reinforcement details similar to experimental work are shown in Figure 10. Also, Figure 10 shows the two steel rollers that are used to connect the tops of the columns of the main frame as reported in the experiment work to prevent the horizontal movement of the columns. Vertical movements of

the columns are not restricted. Also, a 10mm-thick steel plate is fastened above the middle joint to make the load uniformly distributed on the columns. The top and bottom longitudinal bars in beam are anchored with a mechanical anchor to simulate continuity in external beam column joints, as it is in the full-scale specimen.

As reported in the experiment, the numerical simulation of the gradual failure of the middle column stub is performed in a displacement controlled manner as follows; the self-weight of the structural components applied first with all columns support are fixed. Then, a vertical static displacement of the node above column stub is increased gradually to simulate the column failure and the support for this column stub only becomes free. The loading increment is thus defined as 1.0 mm per step (310 steps).

4.3.3 Results and discussions

Figure 11 shows a comparison of crack pattern due to vertical displacement of middle joint equal to 170 mm for scaled specimen (just before rebar fracture) with that obtained from numerical model in the same step. Figure 12 compares the final crack patterns for scaled specimen and the numerical model in ELS. It should be noted that, Figures 11 and 12 indicate that ELS has a great capability to simulate the cracking pattern at each stage.

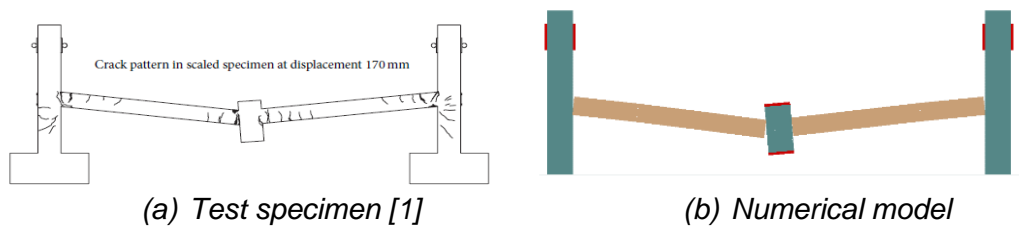


Fig. 11 Crack pattern in scaled specimen at 170 mm vertical displacements of middle Joint

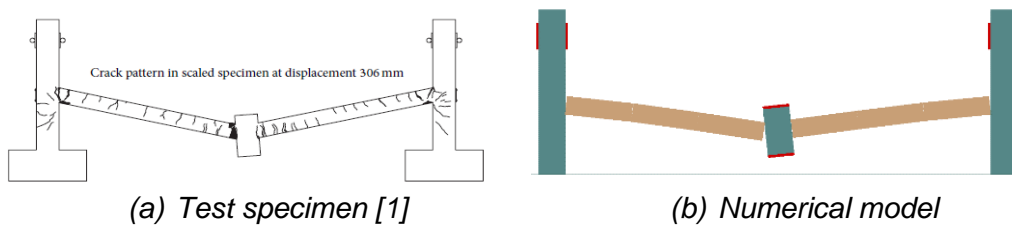


Fig. 12 - Comparison of crack pattern in scaled specimen at the end of test

Similarly, Figure 13 shows images of the bottom rebar fractures at the middle joint interface for both of scaled specimen and ELS. Figures 14 and 15 show images of the top rebar fractures at the side of south column interface for both scaled specimen and ELS. From these figures, it can be concluded that, ELS is capable to simulate rebar fractures very well.



Fig. 13 - Fracture of bottom bars at middle joint

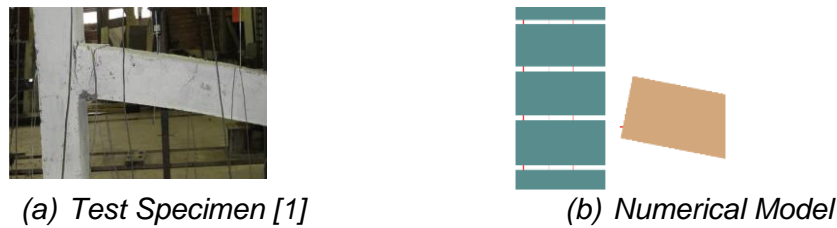


Fig. 14 - Crack pattern at south end

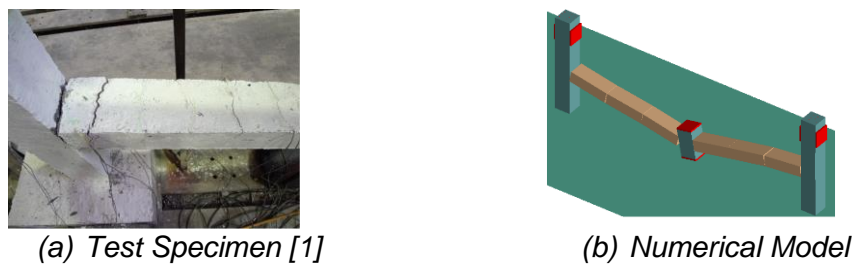


Fig. 15 - Crack pattern at south end

The load-displacement curves from experimental test, OpenSees numerical model, and ELS numerical model are shown in Figure 16. The three mechanisms that resist progressive collapse; flexural action, compressive arch action (CAA) and catenary action (CA) have occurred. As the lower and upper reinforcement at the middle and end joints are yielded quickly during the initial loading steps. Thus, plastic hinges in the beam are created which show that flexural action had reached its capacity at a vertical displacement of 48.3 mm (50 mm in experiment), which is close to half of the beam depth. The load reaches an initial peak of 27.9 kN (28.1 kN in experiment). This point corresponds to the compressive arch action (CAA) capacity of the beams and it can be noticed that, there is no separation point between flexural action and compressive arch action because the compressive arch action is developed at the beginning of the loading in axially restrained members. With additional increments in the vertical displacement, the vertical load started to decrease, and continued to do so until a vertical displacement of 133 mm (135 mm in experiment), which corresponded to a vertical load of 15.5 kN (20.9 kN in experiment) which is approximately equal to the beam depth. Beyond this point, the development of tensile force in the beams leads to increased vertical load capacity. This point is considered as the initiation of increasing the capacity due to catenary action (CA) mechanism of the in-plane frame. Increasing displacement up to 167 mm (170 mm in experiment), increased the vertical load resulting in the first fracture in the lower longitudinal bar in the beam which caused a sudden drop in the load from 20.46 kN to 9.7 kN (22.4 kN to 12.9 kN in experiment). The first rebar fracture occurred at the location of the main crack in the south beam at the interface with the middle column stub. With increasing the displacement, the load started to increase again until the fracture of second bottom bar occurred at displacement of 238 mm (230 mm in experiment) and load value of 33 kN (25.7 kN in experiment). Applying load was stopped with the fracture of one of the beam top bars at the south beam column connection at displacement of 265.5 mm (306 mm in experiment) and load value of 35.5 kN (38.2 kN in experiment), which attained a maximum for CA capacity. Also, it can be observed that there is a large difference in displacement between the stage of bottom bar fracture (at the middle joint) and top bar fracture (at the ends). This can be related to the formation of plastic hinges at the middle joint, which caused large deflections at that stage.

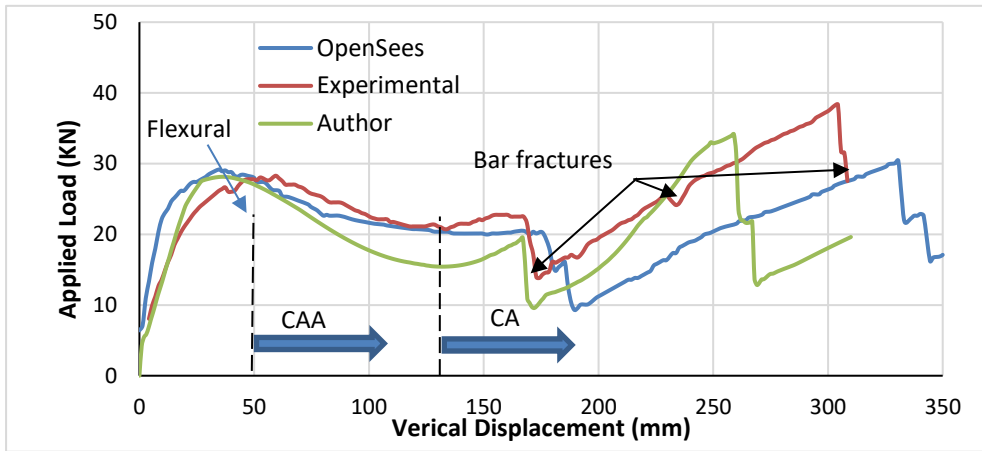


Fig. 16 - Numerical and experimental vertical load-deflection curves

Horizontal displacements of end columns at the beam mid heights which change from inward to outward direction at the vertical displacement of 171 mm (182 mm in experiment) are shown in Figure 17. Also, it can be observed the same behaviour in Figure 18, that shows beam axial force versus vertical displacement of middle joint. The beam axial compression force increased up to vertical displacement of 50 mm and then it started to decrease. In vertical displacement of 171 mm (182 mm in experiment), beam axial force changed from compression to tension and this was evident for development of tensile force in the beams of sub-assembly. This point is considered as the initiation of increasing capacity due to CA mechanism.

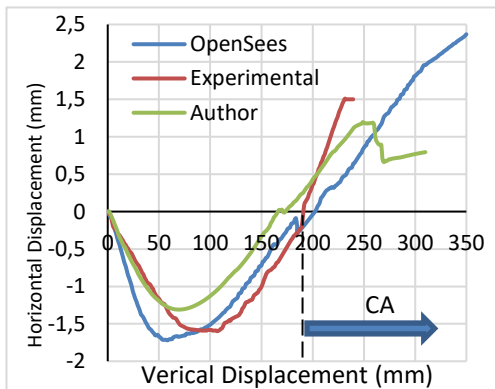


Fig. 17 - Horizontal displacement of end columns versus vertical displacement of center column

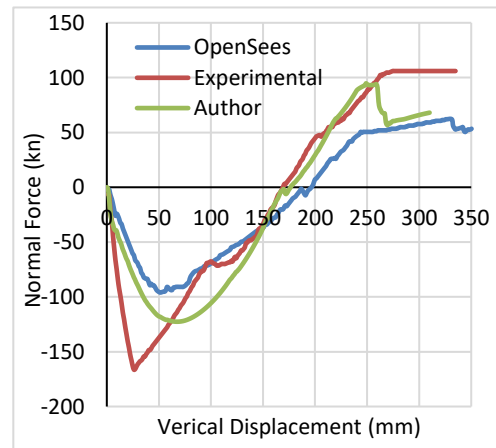


Fig. 18 - Axial force in beam

Strain results at mid span for top and bottom bars are shown in Figures 19 and 20. Generally, the development of strains in the numerical model is the same with experimental scaled specimen. However, the absolute value of strains cannot be modelled because of discrepancies of material properties and stress concentrations in the experimental program. Consequently, it can be concluded that, experimental and numerical results have better agreement especially before the fracture of bars.

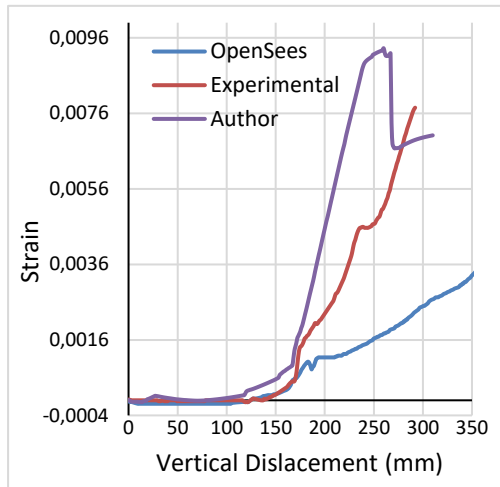


Fig. 19 - Strain in top reinforcing bar at mid-span of the beam

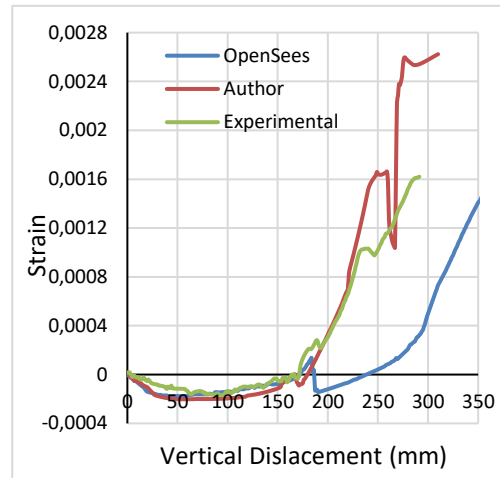


Fig. 20 - Strain in bottom reinforcing bar at mid-span of the beam.

From the above discussion, it should be noted that the numerical model shows better agreement for both vertical and horizontal displacement of the sub-assembly during collapse. Therefore, it is confirmed that AEM can be reliably used to study the progressive collapse of reinforced concrete frames. Furthermore, the results obtained from ELS are even better than those obtained by Ahmedi et al. [1] using OpenSees program.

4.4 Experiment work by Yi et al. [2]

4.4.1 Experiment description

Yi et al. [2] carried out a static experimental study of a three-storey RC frame structure to investigate progressive failure due to the loss of a lower storey column. In their experiment, it was observed that after the plastic mechanism has formed, the concrete strain in the compression zone at the beam ends reached its ultimate compressive strain, and the compressive steel bars are gradually subjected to tension with increasing displacement. For the experimental test, a one-third scale model representing the lower three-story of the original frame from the eight-story RC building was constructed as shown in Figure 21. The dimensions and the reinforcement details of the structural components are shown in Figure 21. Also, the measured material properties are given in Tables 3 and 4.

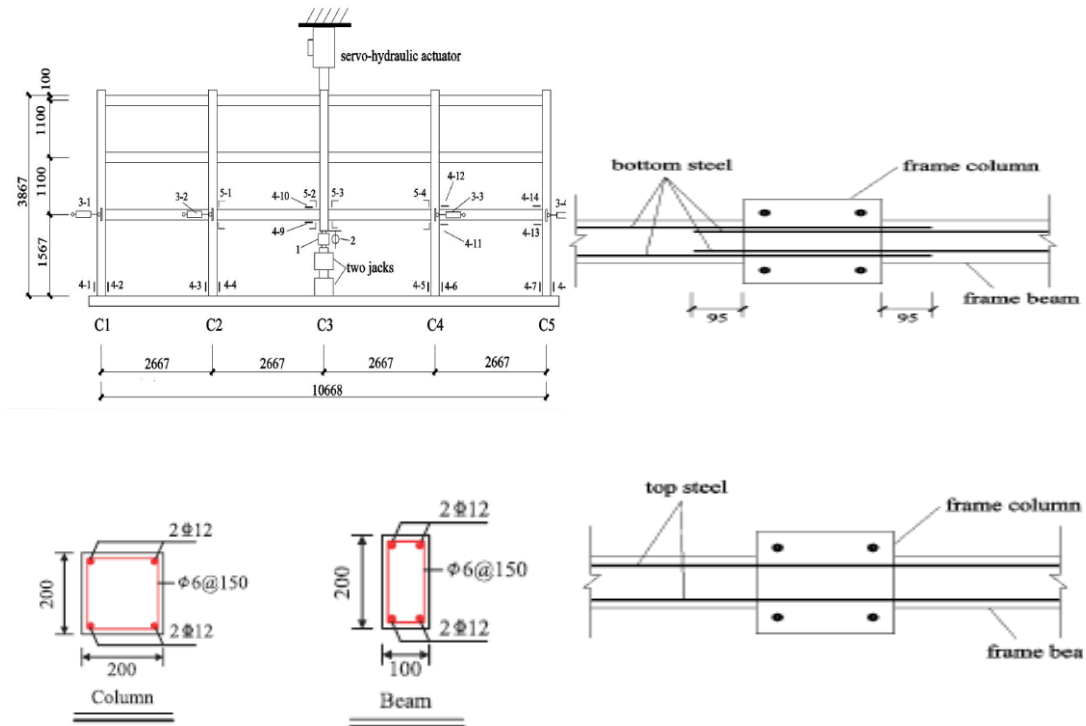


Fig. 21 - Specimen details (Yi et al. [2])

Tab. 3 - Concrete material properties (Yi et al. [2])

Property	Young's Modulus (MPa)	Shear Modulus (MPa)	Tensile Stress (MPa)	Cubic Compressive Stress (MPa)	Specific Weight (Kg/m ³)	Ultimate Strain
Concrete	2.70E4	1.1287E4	1.57	25	2500	0.30

Tab. 4 - Reinforcement material properties (Yi et al. [2])

Property	Young's Modulus (MPa)	Shear Modulus (MPa)	Tensile Yield Stress (MPa)	Compressive Yield Stress (MPa)	Specific Weight (Kg/m ³)	Ultimate Strain
Longitudinal RFT (HRB400)	2.01 E5	0.79 E5	416	416	7840	0.275
Lateral RFT (HPB235)	2.01 E5	079 E5	370	370	7840	0.325

4.4.2 Numerical modelling

Numerical model, mesh division, and reinforcement details similar to experiment are shown in Figure 22.

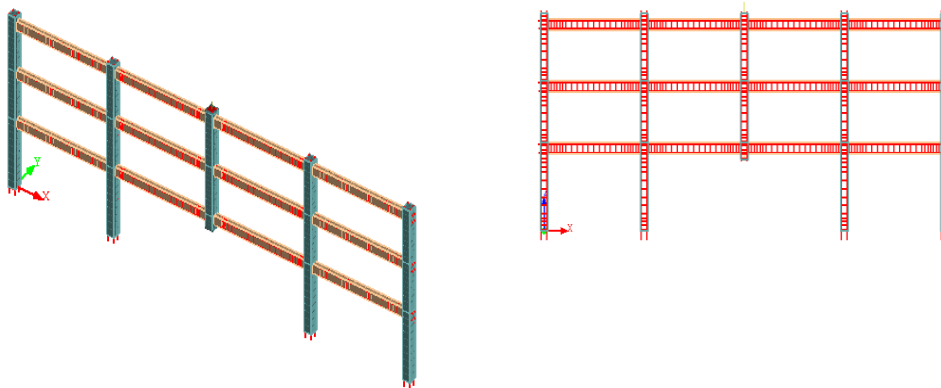


Fig. 22 - ELS Numerical model and reinforcement details

The numerical simulation of the gradual failure of the first-storey middle column is performed in a displacement controlled manner as follows; the self-weight of the structural components applied first then a vertical load of 109 KN is applied incrementally on the top of the middle column, the node associated to the failed column was fixed. After that, a vertical static displacement of this node is increased gradually to simulate the column failure. The loading increment is thus defined as 1.0 mm per step for all models (460 steps).

4.4.3 Results and discussion

It can be noted from Figure 23 that at a vertical displacement less than 5 mm, the elastic stage ended with the cracking of the frame beams. Then, increasing displacement to less than 25 mm, the elasto-plastic stage finishes in point with the yielding of the steel bars from the ends of the beams adjacent to the middle column indicating the formation of the plastic hinge mechanism. After that, increasing the displacement to 140 mm the plastic stage ended where, as in the experiment, large plastic rotations at beams ends and severe concrete crushing are observed in the numerical simulation. After this point the tension cracks in concrete penetrate the compressive zone which means that catenary action stage starts to appear, in which the general resisting mechanism changes from compression bending in beams to tension-bending. Therefore, in this stage the beams are acting mainly as ties. Finally, with increasing the displacement to 450 mm (similar with 456 mm from the experiment), the bottom rebar of the first-storey beam adjacent to the middle column is ruptured. The location of the ruptured rebar from the experiment and the numerical model are illustrated in Figure 24.

Moreover, Figure 23 shows the three stages of mechanism of progressive collapse as first, the adjacent frames are pushed and move outward, second the adjacent frames start being pulled inside, and finally the adjacent frames are pulled inside but the axial force in beams changes to tension. This is happened when the vertical displacement at the column removed point measures 140 mm indicating the formation of the catenary mechanism. Furthermore, comparison of the vertical resisting force versus vertical displacement of the central column obtained in this study with the results obtained by other researchers is shown in Figure 23. This comparison indicated that, the present work simulation is more efficient than other researchers even some of them use the same software and others use different software packages such as; OpenSees, Ansys, Abacus, and MSC Marc.

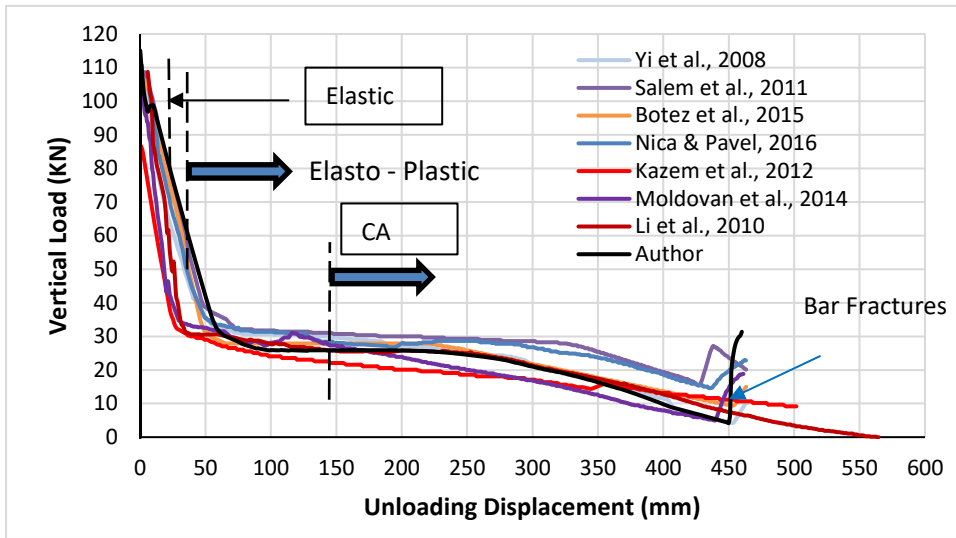
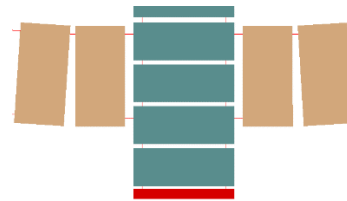


Fig. 23 - Comparison of load-deflection curves



(a) Test specimen (Yi et al. [2])



(b) ELS Model

Fig. 24 - Fracture of bottom bars at middle joint

Figures 25 and 26 present the variation of the vertical and horizontal displacements of sections 3-1 (see Figure 21) obtained from both experimental and numerical work. Also, Figure 27 shows the better simulation for the final deformation of the frame in ELS model with that in the experiment.

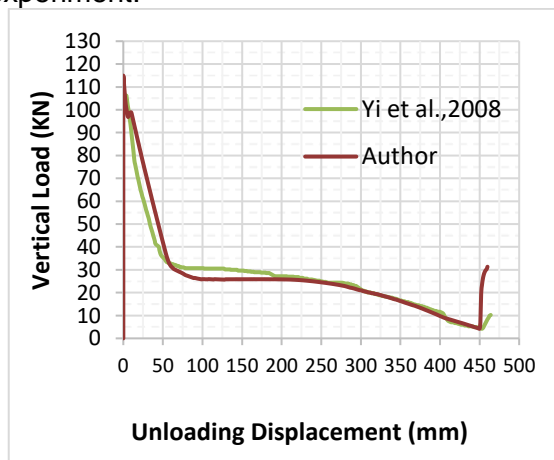


Fig. 25 - Vertical load-deflection results

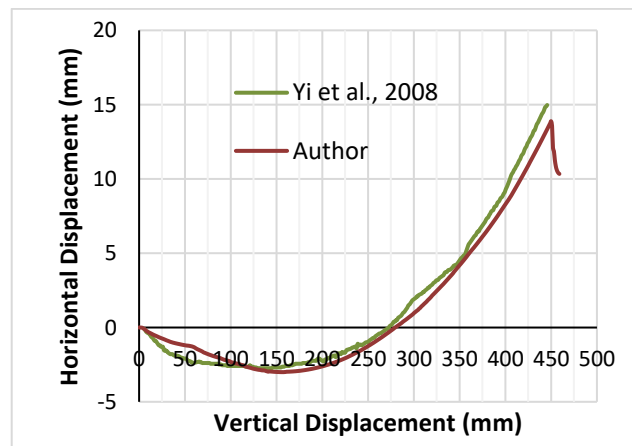
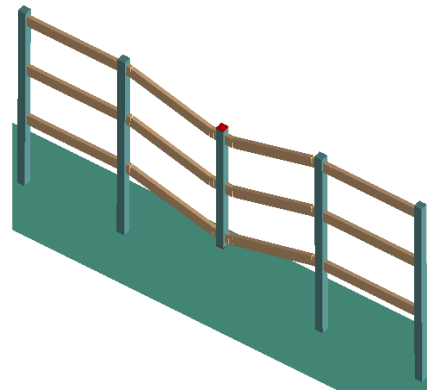


Fig. 26 - Horizontal displacement of end columns versus vertical displacement of center column



(a) Test specimen (Yi et al. [1])



(b) ELS model

Fig. 27 - Frame final deformation

5. CONCLUSION

In this study, a numerical investigation is conducted using ELS software (Extreme Loading for Structures) which is based on the Applied Element Method (AEM) based on an experimental data of the two experimental studies conducted by Ahmadi et al. [1] and Yi et al. [2]. The numerical modelling results are compared with those obtained from experiments as well as other software packages such as OpenSees, Ansys, Abacus and MSC Marc. The main findings in this study can be summarized as follows:

1. The applied element method is an efficient tool for analysis of progressive collapse of reinforced concrete structures.
2. The numerical results obtained using ELS show a better agreement with experimental results.
3. ELS has a great capability to simulate both the crack pattern in each stage and rebar fractures.
4. There is no separation point between flexural action and compressive arch action because the compressive arch action developed at the beginning of the loading in axially restrained members.
5. The transition point from compressive arch action to catenary action occurred only when axial loads changed from a compression force to a tension force.
6. The ELS software could be utilized in further progressive collapse analyses.
7. The developed numerical model is regarded a valid and economical alternative to experiments for prediction of the progressive collapse of reinforced concrete structures.

ACKNOWLEDGEMENTS

The authors acknowledge *Benha University* for its effort to provide us with all scientific papers and references needed to complete this research. Also, the authors would like to thank Eng. *Mahmoud Abbas*, Teaching Assistant, *Civil Engineering Department, Faculty of Engineering at Shoubra, Benha University* for support in modelling by ELS.

REFERENCES

- [1] Ahmadi, R., Rashidian, O., Abbasnia, R., Mohajeri Nav, F. and Yousefi, N., "Experimental and Numerical Evaluation of Progressive Collapse Behavior in Scaled RC Beam–Column Sub-Assemblage", *Shock and Vibration*, doi:10.1155/2016/3748435, 2016.
- [2] Yi, W.J., He, Q.F., Xiao Y., Kunnath, S.K., "Experimental Study on Progressive Collapse-Resistant Behavior of Reinforced Concrete Frame Structures", *ACI Struct J*, 105(4):433-439, 2008.
- [3] American Society of Civil Engineers (ASCE), "Minimum Design Loads for Buildings and Other Structures (SEI/ASCE 7/05).", Reston Va., USA, 2005.
- [4] General Service Administration, GSA, "Progressive Collapse Analysis and Design Guidelines for New Federal Office Buildings and Major Modernization Projects"; Washington DC, 2003.
- [5] Nair R.S., "Preventing Disproportionate Collapse," *Journal of Performance of Constructed Facilities* ASCE, vol. 20(4), pp. 309–314, 2006.
- [6] Ellingwood, B. R. and Dusenberry D. O., "Building Design for Abnormal Loads and Progressive Collapse", *Computer-Aided Civil and Infrastructure Engineering*, 20:194–205, 2005.
- [7] Interagency Security Design Committee (ISC), "Criteria for New Federal Office Buildings and Major Reorganization Projects", 2001.
- [8] Structural Use of Steelwork in Building, Part 1: Code of Practice for Design - Rolled and Welded Sections, British Standards Institute, (BS 5950-1), 2000.
- [9] Department of Defense, DoD, "Design of Buildings to Resist Progressive Collapse", Unified Facilities Criteria (UFC, 4-023-03). USA; 2005 & 2009.
- [10] Meguro, K. and Tagel-Din, H., "Applied Element Method for Structural Analysis: Theory and Application for Linear Materials", *Structural Engineering Earthquake Engineering, International Journal of the Japan Society of Civil Engineers (JSCE)* 17(1):21s–35s, 2000.
- [11] Meguro, K. and Tagel-Din, H., "Applied Element Simulation of RC Structures Under Cyclic Loading", *Journal of Structural Engineering*, 127(11):1295–1305, 2001.
- [12] Meguro, K. and Tagel-Din, H., "Applied Element Method Used for Large Displacement Structural Analysis", *Journal of Natural Disaster Science*, 24(1):25–34, 2002.
- [13] Tagel-Din, H. and Meguro, K., "Applied Element Simulation for Collapse Analysis of Structures", *Bulletin of Earthquake Resistant Structure Research Centre, IIS, University of Tokyo*, pp. 113–123, 1999.
- [14] Tagel-Din, H. and Meguro, K., "Analysis of a Small-Scale RC Building Subjected to Shaking Table Tests Using Applied Element Method", *Proceedings of the 12th World Conference on Earthquake Engineering, New Zealand*, pp. 1–8, 2000a.
- [15] Tagel-Din, H. and Meguro, K., "Applied Element Method for Dynamic Large Deformation Analysis of Structures", *Structural Engineering Earthquake Engineering*, 17(2):215s–224s, 2000b.
- [16] Applied Science International, Durham, NC, "Extreme Loading for Structures - Theoretical Manual", 2013.
- [17] Ramancharla, P.K., Tagel-Din, H. and Meguro, K., "Dynamic Modeling of Dip-slip faults for Studying Ground Surface Deformation Using Applied Element Method", *13th World Conference on Earthquake Engineering*, 2004.
- [18] Mayorca, P. and Meguro, K., "Modeling Masonry Structures Using the Applied Element Method", *Seisankenkkyu*, 55(6):581–584, 2003.
- [19] Asprone, D., Nanni, A., Salem, H. and Tagel-Din, H., "Applied Element Method Analysis of Porous GFRP Barrier Subjected to Blast", *Advances in Structural Engineering*, 13(1):153–170, 2010.
- [20] Coffield, A. and Adeli, H., "An Investigation of the Effectiveness of the Framing Systems in Steel Structures Subjected to Blast Loading", *Journal of Civil Engineering and Management*, 20(6):767–777, 2014.
- [21] Applied Science International, Durham, NC, "Extreme Loading for Structures V3.1 - Modeling Manual", April 2010.
- [22] Okamura, H. and Maekawa, K., "Nonlinear Analysis and Constitutive Models of Reinforced Concrete", Gihodo Co. Ltd., Tokyo, 1991.
- [23] Kupfer, H., Hilsdorf, H.K. and Rusch, H. "Behavior of Concrete under Biaxial Stresses", *Proceeding of ACI Journal*, volume 66-8., 656-666, 1969.

- [24] Ristic, D., Yamada, Y. and Iemura, H., "Stress-Strain Based Modeling of Hysteretic Structures Under Earthquake Induced Bending and Varying Axial Loads", Research Report No. 86-ST-01. Kyoto (Japan): School of Civil Engineering. Kyoto University, 1986.
- [25] Galal K and El-Sawy T., "Effect of Retrofit Strategies on Mitigating Progressive Collapse of Steel Frame Structures", *J Construct Steel Res* 2010;66(4):520–31.
- [26] Sasani, M., "Response of a Reinforced Concrete Infilled-Frame Structure to Removal of Two Adjacent Columns", *Engineering Structures*, 30, 2478-2491, 2008.
- [27] Wibowo, H., Reshotkina, S. S. and Lau, D. T., "Modelling Progressive Collapse of RC Bridges During Earthquakes", CSCE Annual General Conference May 27-30 2009 St. John's, NL, Canada.
- [28] Tagel-Din, H. and Rahman, N., "Extreme Loading: Breaks Through Finite Element Barriers", *Struct Eng* 2004;5(6):32–40.
- [29] Tagel-Din, H. and Meguro, K., "Applied Element Method for Simulation of Nonlinear Materials: Theory and Application for RC structures", *Struct Eng Earthquake Eng Int J Jpn Soc Civil Eng (JSCE)* 2000;17(2):123s–48s.
- [30] Salem H., "Computer-Aided Design of Framed Reinforced Concrete Structures Subjected to Flood Scouring", *Journal of American Science*, 7, 191-200, 2011.
- [31] Tagel-Din, H., "Collision of Structures During Earthquakes", *Proceedings of the 12th European Conference on Earthquake Engineering*, 2002, London, UK.
- [32] Meguro, K. and Tagel-Din, H., "AEM Used for Large Displacement Structure Analysis", *Journal of Natural Disaster Science*, 2003, 24 (1), 25-34.
- [33] Park H, Suk C. and Kim, S., "Collapse Modeling of RC Structures using the Applied Element Method", *Journal of Korean Society for Roc Mechanics, Tunnel & Underground Space*, 2009, 19 (1), 43-51.
- [34] Helmy, H., Salem, H. and Tageldin, H., "Numerical Simulation of Charlotte Coliseum Demolition using the Applied Element Method", *USNCCM-10 conference-Ohio-USA*, 2009.
- [35] Helmy, H., Salem, H. and Mourad, S., "Progressive Collapse Assessment of Framed Reinforced Concrete Structures According to UFC Guidelines for Alternative Path Method", *Engineering Structures*, 2012, 42, 127–141.
- [36] Helmy, H., Salem, H. and Mourad, S., "Computer-Aided Assessment of Progressive Collapse of Reinforced Concrete Structures According to GSA Code", *Journal of Performance of Constructed Facilities*, ASCE, October 2013.
- [37] Salem, H. and Helmy, H., "Numerical Investigation of Collapse of the Minnesota I-35W Bridge", *Engineering Structures*, 2014, 59, 635–6.
- [38] Salem, H. M., El-Fouly, A. K. and Tagel-Din, H. S., "Toward An Economic Design of Reinforced Concrete Structures Against Progressive Collapse", *Engineering Structures*, 33, 3341-3350, 2011.
- [39] Salem, H., Mohssen, S., Kosa, K., and Hosoda, A., "Collapse Analysis of Utatsu Ohashi Bridge Damaged by Tohoku Tsunami using Applied Element Method", *Journal of Advanced Concrete Technology*, 2014, Vol. 12(10), 388-402.
- [40] Lupoae, M. and Bucur, C., "Use of Applied Element Method to Simulate the Collapse of a Building", *SISOM 2009 and Session of the Commission of Acoustics*, Bucharest 28-29 May.
- [41] Lupoae, M., Baciuc, C., Constantin, D. and Puscau, H., "Aspects Concerning Progressive Collapse of a Reinforced Concrete Frame Structure with Infill Walls", *Proceedings of the World Congress on Engineering*, WCE 2011. London, U.K.
- [42] El-Mahdy, O., El-Kasaby, E., Abusafa, H., and El-Gamal, A., "Application of AEM in Progressive Collapse Dynamics Analysis of R.C. Structures", *The Civil Engineering Journal (CEJ)*, Stavebni Obzor, Faculty of Civil Engineering, CTU in Prague, Czech Republic, October 2017
- [43] MC2010, FIP, "Model Code for Concrete Structures", Ernst & Sohn.
- [44] ACI 318-02, "Building Code Requirements for Structural Concrete and Commentary", American Concrete Institute, 2002.
- [45] Botez M., Bredean L., Ioani A., "Improving the Accuracy of Progressive Collapse Risk Assessment: Efficiency and Contribution of Supplementary Progressive Collapse Resisting Mechanisms", *ComputStruct*; DOI: 0.1016/j.compstruc.2015.11.002.

- [46] Nica, G.B. and Pavel, F., "Numerical Analysis of the Collapse of a RC Frame", *Mathematical Modelling in Civil Engineering Journal*, Vol. 12-No. 4, pp.22 - 35, 2016
- [47] Moldovan, T.S., Marchiş, A.G. and Ioani, A.M., "Progressive Collapse Analysis of an Old RC Structure Subjected to Extreme Loading", *International Scientific Conference, People, Buildings and Environment 2014*, Kroměříž, Czech Republic, pp. 316-327, ISSN: 1805-6784.
- [48] Li, Y., Lu, X., Guan H. and Ye, L., "An Improved Tie Force Method for Progressive Collapse Resistance Design of Reinforced Concrete Frame Structures", *EngStruct*, 33:2931-2942, 2011.
- [49] Kazem, A., Kazem, H. and Monavari, B., "Effect of Progressive Collapse in Reinforced Concrete Structures with Irregularity in Height", *15 WCEE*, Lisboa, 2012.
- [50] Tagel-Din, H. and Meguro, K., "Nonlinear Simulation of RC Structures Using Applied Element Method", *Structural Engineering Earthquake Engineering*, 17(2):137s–147s, 2000c.